Regular Article

PHYSICAL CHEMISTRY RESEARCH
Published by the
Iranian Chemical Society
www.physchemres.org
info@physchemres.org

*Phys. Chem. Res., Vol. 11, No. 3, 589-604, September 2023*
**DOI: 10.22036/pcr.2022.349693.2138**

# *In Silico* Approach for Designing Novel SARS-CoV-2 Inhibitors from Medicinal Plants

R.T. Fouedjou[a], O. Daoui[b], H. Nour[c], M. Ayoub[d], H.P.D. Fogang[e], F. Siddique[d], S. Elkhattabi[b], M. Bakhouch[f], S. Belaidi[g] and S. Chtita[c,*]

[a]*Research Unit of Environmental and Applied Chemistry, Department of Chemistry, Faculty of Science, University of Dschang, Box 67, Dschang, Cameroon*

[b]*Laboratory of Engineering, Systems, and Applications, National School of Applied Sciences, Sidi Mohamed Ben Abdellah-Fez University, BP Box 72, Fez, Morocco*

[c]*Laboratory of Analytical and Molecular Chemistry, Faculty of Sciences Ben M'Sik, Hassan II University of Casablanca, B.P 7955, Casablanca, Morocco*

[d]*Department of Pharmaceutical Chemistry, Faculty of Pharmacy, Bahauddian Zakariya University, Multan 60800 Pakistan*

[e]*Department of Physiological Sciences and Biochemistry, Faculty of Medicine and Biomedical Sciences of Garoua, University of Garoua, Garoua, Cameroon*

[f]*Laboratory of Bioorganic Chemistry, Department of Chemistry, Faculty of Sciences, Chouaïb Doukkali University, P.O. Box 24, 24000 El Jadida, Morocco*

[g]*Group of Computational and Medicinal Chemistry, LMCE Laboratory, University of Biskra, Biskra, Algeria*

*(Received 14 July 2022, Accepted 8 September 2022)*

Several countries in the world, are still under the threat of SARS-CoV-2 propagation, although the majority of the population has received a vaccine. Some ethno-botanical surveys were conducted to document potential herbal remedies that can be used in the management of the COVID-19 pandemic in Cameroon. Medicinal plants belonging to Cameroon flora could be a source for the discovery of potential inhibitors of SARS-CoV-2 $M^{pro}$ and spike proteins. These two proteins play a pivotal role in mediating viral replication and transcription, making them attractive targets for drug design against SARS-CoV-2. The aim of this in silico study is to evaluate the behavior of the isolated secondary metabolites from Cameroonian medicinal plant species towards SARS-CoV-2 $M^{pro}$ and spike proteins. In the present study, six plant species are selected among the frequently used plants to treat COVID-19 and related symptoms in Cameroon. To highlight the interactions of studied secondary metabolites with SARS-CoV-2 $M^{pro}$ (6lu7) and spike (6m0j) proteins a molecular docking analysis is used. Among the one hundred and twenty-five screened compounds, thirty-five showed high binding affinity against the two targeted proteins. Furthermore, molecular dynamics simulations were performed to support the docking results. Additional investigations, including physicochemical properties, pharmacokinetics, and toxicological profile show that only twelve compounds bind tightly to $M^{pro}$ (6lu7) and spike (6m0j) proteins and could be considered as promising drug candidates of SARS-CoV-2. The selected twelve compounds are evaluated for their acute and chronic toxicity, possible mutagenic, tumorigenic, irritant, and reproductive effectiveness. The outcomes of this study suggest the possibility of developing potent $M^{pro}$ and spike proteins inhibitors from naturally occurring compounds belonging to Cameroon flora.

**Keywords:** Natural products, Cameroon flora, SARS-CoV-2, $M^{pro}$, Spike protein, Molecular docking, Molecular dynamics, ADME-Tox

## INTRODUCTION

COVID-19 has spread worldwide hitting some countries with extreme cruelty. The agent of this disease namely SARS-CoV-2 or 2019 novel coronavirus (2019-nCov) was identified as a new strain of coronavirus [1]. According to WHO, 216 countries and territories around the world have reported more than 74.30 million confirmed COVID-19

*Corresponding author. E-mail: samirchtita@gmail.com

cases with a death toll of above 1.67 million [2]. To date, even though some vaccines have been approved, the search for new drugs to fight this pandemic is still ongoing. Like many viruses, coronavirus exploits the extensive network of its host cell's signaling pathways to promote viral replication and propagation [3,4]. This dependence on protein-protein interactions offers the unique opportunity to target both viral-host and intraviral protein-protein interactions and, thereby, stop viral replication and propagation.

The coronaviral genome encodes four major structural proteins: the spike (S) protein, nucleocapsid (N) protein, the main protease ($M^{Pro}$), and the envelope (E) protein, all of which are required to produce a structurally complete viral particle [5-7]. Before being involved in other aspects of the replication cycle, each protein primarily plays a role in the structure of the virus particle. The S protein mediates attachment of the virus to the host cell surface receptors and subsequent fusion between the viral and host cell membranes to facilitate viral entry into the host cell [8-10]. This interaction has been proposed as a strategy to allow the direct spreading of the virus between cells, subverting virus-neutralizing antibodies [11-13]. The $M^{pro}$ is the most abundant structural protein and defines the shape of the viral envelope [14]. It is also regarded as the central organizer of CoV assembly, interacting with all other major coronaviral structural proteins [15]. Interdependence of S with $M^{pro}$ is necessary for retention of S in the ER-Golgi intermediate compartment ERGIC/Golgi complex and its incorporation into new virions, but dispensable for the assembly process [5, 11,16]. These few details support our choice of SARS-CoV-2 $M^{pro}$ coded PDB ID: 6lu7 and spike protein coded PDB ID: 6m0j for this study.

To contribute to the search for a potential solution for COVID-19, we have carried out an *in-silico* study on some naturally occurring compounds isolated from Cameroonian medicinal plants known for their therapeutic effects [17]. It is important to remind that, therapies that use small molecules as drugs have the advantage to cross cell membranes efficiently. These kind of molecules have also several limits such as selectivity and targeting capabilities, which often leads to undesired side effects [18].

For this study, six medicinal plants from different families have been selected. The first, *Daucus carota* L. belongs to the Apiaceae family, commonly known as wild carrot, is widely used in nutrition and as a dietary supplement in Cameroon [19]. This plant is an important source of bioactive compounds with a beneficial effect on consumer health. In addition to the anticancer activity of $\beta$-carotene which is its major constituent and the precursor of vitamin A, it is recognized as an important source of natural antioxidants [20]. Moreover, *Daucus carota* leaf and root are diuretic, useful for fertility, and effective against cough, pleurisy, corrosive ulcer, and dropsy [21]. The crushed leaves of *Daucus carota* are introduced in a container and the volume is completed to 5L with palm wine or raffia wine to treat HIV/AIDS [22].

The second plant, *Millettia griffoniana* (Fabaceae), appears in the African pharmacopeia for centuries. It has a wide range of biological activities such as antitumoral, anti-inflammatory, antiviral, bactericidal, insecticidal, and pest-destroying [23]. The multiplicity of these activities confers to this plant a great interest in traditional medicine as well as in the research of new biologically active compounds. *Millettia griffoniana* is among the 14 plant species known in Cameroon for its antiviral properties against virus-induced diseases [24].

The third plant, *Aframomum danielli* (Hook.f.) Schum, is a member of the family Zingiberaceae. It inhibits the growth of *Salmonella enteriditis*, *Staphylococcus aureus*, *Aspergillus flavus*, *Aspergillus parasiticus*, and *Aspergillus ochraceus* [25]. *Aframomum danielli* also inhibits the growth of *Listeria* monocytogenes [26], protects liver cells [27], kills filariasis mosquitoes larva's [28], and possesses scavenging capacities [29].

The fourth plant, *Rauwolfia vomitoria* Afz*.,* belongs to the family Apocynaceae. Major phytochemical constituents of this plant include alkaloids, glycosides, polyphenols, and reducing sugars [30]. Traditionally, *Rauwolfia vomitoria* are used to manage ailments such as mental disorders, hypertension, dysentery, jaundice, cerebral cramps, and gastrointestinal disorders [31]. Research reports showed that the plant has antioxidant, antipyretic, antiglycemic, anticonvulsant, analgesic, antipsychotic, and sedative properties [32-34].

*Eucalyptus globulus*, the fifth plant selected, is known for its richness of bioactive compounds such as essential oils, phenolic acids, flavonoids, and hydrolysable tannins [35-38].

The last plant, *Acanthus montanus* (Nees) T. Anderson of the Acanthaceae family is a quick-growing evergreen herb distributed mainly in the tropical region. In Traditional Medicine and Pharmacopoeia of Cameroon, *Acanthus montanus* is known to treat for pain, cough, epilepsy, dysmenorrhea, miscarriages, and false labor [39,40].

## MATERIALS AND METHODS

### Database

A set of 125 compounds have been identified from an extensive literature search conducted on *D. carota*, *M. griffoniana*, *A. daniellii*, *R. vomitoria*, *E. globulus* and, *A. montanus*. Discovery Studio 2020 software was used to convert the structures of studied compounds into a single database format (sdf). The ligands file was read in AutoDock 2.1.4 under full protonation mode and converted to the most energy-stable structure. After the optimization of the top candidates, we furthermore, conducted a molecular docking analysis of the top candidates with potential therapeutic targets for the inhibition of SARS-CoV-2 replication.

### Targets Retrieval and Preparation

The three-dimensional structure of SARS-CoV-2 $M^{pro}$ protein in complex with the covalent peptide N3 was downloaded from Protein Data Bank (PDB) database (www.rcsb.org) with the code 6lu7 [41]. The grid box dimensional was 20*20*20 (x, y, z), with the center of (x = -10.641, y = 11.847, z = 68.346) to suit the binding site of the removed N3 inhibitor. The same steps were applied for spike protein (6m0j), with difference of grid box options with a size of (x = 24, y = 24, z =24) and a center of (x = -34.933, y = 8.672, z = 29.036. Both proteins were ready to perform molecular docking by applying the last steps. The grid center corresponds to the coordinates: x = -26.283, y = -12.599, and z = 58.965, the grid boxes were placed at the binding site of the enzymes, which give sufficient space for the ligand rotation and translation [42,43]. Giving to the results of recent molecular mechanics investigations, Nelfinavir was chosen as a reference ligand with both SARS-CoV-2 $M^{Pro}$ (6lu7) and spike proteins (6m0j) [44,45].

### Virtual Screening

In order to show the bounding modes of ligands with target proteins, molecular docking was therefore performed for 125 phytoconstituents with both SARS-CoV-2 $M^{Pro}$ and spike proteins. Polar hydrogen atoms were added and constrained during the docking process and all the torsional bonds of ligands were freed by using the ligand module in AutoDock Tools (ADT) [46]. The results were expressed according to the binding energy value, and the molecule with the lowest binding energy was considered to be the best one to interact with the target protein.

### Properties and Pharmacokinetic Profile of Top Candidates

Physicochemical properties (molecular weight, H-bonding, heavy atoms, water solubility, *etc*.), pharmacokinetics (Gastrointestinal absorption, bioavailability score, permeability, interaction of molecules with cytochromes P450 (CYP), elimination route, …*etc*.), and low cost of production are evaluated as a basic step in the drug discovery process. The chemical structure of the potential candidates was submitted in the form of a canonical simplified molecular input line entry system (SMILES), to estimate several *in silico* pharmacokinetic parameters using the Swiss ADME tool [47]. The toxicological profile, based on the ProTox-II16 online web server (https://tox-new.charite.de/protox_II) of the potential candidate was examined to guarantee their safety. This server was used to predict oral toxicity, cytotoxicity, carcinogenicity, immunotoxicity, and mutagenicity effects. Minnow toxicity (MT), Hepatotoxicity (HP), and Skin Sensitization (SS) are also examined.

### Molecular Dynamics Simulations

Molecular dynamics simulations (MD) were performed using GROMACS [48] with charmm27force field [49] to gain insight into the stability of 6lu7 complexed with the best docked compound (sesamin) having shown good pharmacokinetics properties. The topology of sesamin was retrieved from the SwissParam server [50]. Moreover, the 6lu7-sesamin complex was covered by a cubic simulation box and then solvated with TIP3P water molecules. Four sodium ions were added to neutralize the overall system. Following that, the simulated system was optimized using steepest descent minimization to avoid steric clashes. Then, we performed NVT equilibration at 300 K for 1 ns followed

by NPT equilibration utilizing Parrinello-Rahman barostat at 1 atm for 1 ns [51] to stabilize the systems at the desired conditions. Finally, the equilibrated system was subjected to MD for 150 ns. From the simulation results, we calculated various parameters e.g., root mean square deviation (RMSD), root mean square fluctuation (RMSF), Radius of gyration (Rg), number of hydrogen bonds, and Solvent Accessible Surface Area (SASA).

## RESULTS AND DISCUSSION

### Virtual Screening of Ligand with SARS-CoV-2 Proteins Domains and in Silico ADME-Tox Analysis

Chemical ligand database, build on 27 compounds previously isolated from *D. carota*, 21 from *M. griffoniana*, 8 obtained from *A. daniellii*, 36 isolated from *R. vomitoria*, 16 purified from *E. globulus*, and 17 isolated from *A. montanus* was docked using AutoDock Tools1.5.6 software against $M^{pro}$ (6lu7) and spike (6m0j) proteins (Table 1). Relatively, lower binding energy and hydrogen bonding distance were considered to find the most probable docking conformation. The results of docking analysis are described in Table 1, with Nelfinavir as a drug reference. The negative and low value of free energy of binding (between -3.6 and -9.0 kcal $mol^{-1}$) proves the ability of these phytochemical ligands to interact with the selected viral proteins. From these binding free energy values, compounds with good affinity for Coronavirus proteins (6lu7 and 6m0j) were chosen and their pharmacological characteristics were determined.

Table S1 shows 35 compounds with binding energy values ranging from -6.5 to -9.0 kcal $mol^{-1}$, which indicates that these compounds could be of an affinity comparable to that of the Nelfinavir reference (-6.83 kcal $mol^{-1}$). These compounds are Griffonianones A (28), Griffonianone B (29), Griffonianone B methylether (5-methoxydurmillone) (30), Griffonianones C (31), Maximaisoflavone G (32), 7-Hydroxy-6-methoxy-3',4'-methylenedioxyisoflavone (29), Maximaisoflavone G acetate (30), 7-Acetoxy-6-methoxy-3',4'-methylenedioxyisoflavone (35), 7-O-geranylformononetin (36), 3',4'-dihydroxy-7-O-[(E)-3,7-dimethyl-2,6-octadienyl]isoflavone (37), Griffonianone D (38), Griffonianone E (39), 4'-O-geranylisoliquiritigenin (40), 3',4'-methylenedioxy-7-O-[(E)-3,7-dimethyl-2,6-octadienyl] isoflavone (41), calapogonium isoflavone B (42), 7-2'-dimethoxy-4',5'-methylenedioxy isoflavone (43), Jamaicin (44), Durmillone (45), 4'-Methoxy-7-*O*[(E)-3-methyl-7-hydroxymethyl-2,6-octadienyl]isoflavone (47), 4-Hydroxy-5,6,7-trimethoxy-3-(3',4'-methylenedioxy) phenylcoumarin (48) isolated from *M. griffoniana*; Normacusine B (58), Peraksine (vomifoline) (61), Geissoschizine (62), Tetrahydroalstonine (63), Urs-12-en-28-ol, (89), Neonorreserpine (92) isolated from *R. vomitoria*; Sesamin (99), 3β,11α-Dihydroxyurs-12-en-28-oic acid (100), Cypellocarpa C (102), Aromadendrenea (105) isolated from *Eucalyptus globulus* and Acanmontanoside (117), Decaffeoylverbascoside (118), Isoverbascoside (120), Leucosceptoside A (121), Verbascoside (124) from *A. montanus*. Cypellocarpa C (102) exhibited the highest binding affinity with the SARS-CoV-2 $M^{pro}$ (6lu7) protein (-9.0 kcal/mol), while Griffonianones A (28) and Sesamin (99) exhibited the highest binding affinity with the SARS-CoV-2 spike protein (-8.3 kcal $mol^{-1}$).

To gain insight into their mode of recognition, we also analyzed the interactions involved between the target proteins and the compound having shown the highest docking score. The involved interactions are depicted in Fig. 1. As shown in Fig. 1a, the molecular recognition between Sesamin (99) and 6lu7 was performed by involving three hydrogen bonds with HIS41, GLU166, and GLU143, as well as a Pi-alkyl interaction with CYS145. Besides, to accomplish its recognition with 6m0j, Sesamin (99) involved three hydrogen bonds with SER371, TRP436, and VAL367, in addition to Pi-alkyl and Pi-Pi interactions with VAL367 and TRP436, respectively.

### Drug-like and Pharmacokinetics Profiles of Screened Phytochemicals

The interactions and binding of drug candidates to protein receptors can lead to a beneficial or toxic effect. Therefore, the screening of drug candidate molecules for their drug-like properties is an important step in drug discovery. Based on this insight, we performed an *in-silico* screening of the pharmacological properties of the investigated candidate phytochemicals to obtain enough information on the inhibition of SARS-CoV-2 proteins.

The database generated from the virtual screening of the 125 ligands with SARS-CoV-2 proteins allowed us to continue the screening of phytochemicals obtained from four

**Table 1.** *In Silico* Binding Free Energies (kcal $mol^{-1}$) with SARS-CoV-2 $M^{pro}$ (PDB ID: 6lu7) and Spike (PDB ID: 6m0j) Proteins Using Docking Analysis

| Phytochemicals | N° | 6lu7 | 6m0j | | N° | 6lu7 | 6m0j | | N° | 6lu7 | 6m0j |
|---|---|---|---|---|---|---|---|---|---|---|---|
| *Daucus carota* | 01 | -3.6 | -3.6 | *Aframomum daniellii* Hook | 49 | -4.4 | -5.1 | *Eucalyptus globulus* | 97 | -5.1 | -4.5 |
| | 02 | -5.5 | -6.2 | | 50 | -5.4 | -6.3 | | 98 | -7.2 | -6.4 |
| | 03 | -5.9 | -5.7 | | 51 | -5.9 | -5.9 | | 99 | -8.4 | -8.3 |
| | 04 | -5.6 | -5.7 | | 52 | -4.5 | -5.3 | | 100 | -7.1 | -7.0 |
| | 05 | -5.3 | -5.8 | | 53 | -4.3 | -5.1 | | 101 | -6.2 | -6.0 |
| | 06 | -5.9 | -6.0 | | 54 | -4.5 | -5.3 | | 102 | -9.0 | -7.6 |
| | 07 | -5.3 | -6.0 | | 55 | -4.5 | -4.9 | | 103 | -4.3 | -5.2 |
| | 08 | -5.3 | -6.1 | | 56 | -5.2 | -5.4 | | 104 | -5.3 | -5.9 |
| | 09 | -4.9 | -6.1 | *Rauwolfa vomitoria* | 57 | -6.7 | -7.0 | | 105 | -7.3 | -6.7 |
| | 10 | -5.1 | -6.1 | | 58 | -7.7 | -7.7 | | 106 | -6.2 | -5.8 |
| | 11 | -5.0 | -5.4 | | 59 | -6.8 | -6.7 | | 107 | -6.5 | -6.8 |
| | 12 | -5.0 | -5.7 | | 60 | -6.8 | -6.5 | | 108 | -6.7 | -5.9 |
| | 13 | -4.6 | -5.4 | | 61 | -7.5 | -8.0 | *Acanthus montanus* | 109 | -7.1 | -6.2 |
| | 14 | -5.1 | -5.6 | | 62 | -7.5 | -6.6 | | 110 | -4.5 | -3.6 |
| | 15 | -5.8 | -6.2 | | 63 | -6.8 | -7.2 | | 111 | -5.2 | -5.7 |
| | 16 | -6.0 | -6.4 | | 64 | -6.7 | -6.7 | | 112 | -5.3 | -6.3 |
| | 17 | -5.8 | -5.8 | | 65 | -6.6 | -6.6 | | 113 | -4.8 | -5.0 |
| | 18 | -4.6 | -5.2 | | 66 | -7.1 | -6.5 | | 114 | -5.0 | -4.3 |
| | 19 | -4.6 | -5.2 | | 67 | -6.4 | -6.6 | | 115 | -4.8 | -5.2 |
| | 20 | -4.6 | -5.0 | | 68 | -6.8 | -6.2 | | 116 | -4.5 | -5.7 |
| | 21 | -4.6 | -5.2 | | 69 | -7.0 | -6.5 | | 117 | -8.3 | -7.1 |
| | 22 | -5.2 | -6.8 | | 70 | -6.9 | -6.4 | | 118 | -7.7 | -6.8 |
| | 23 | -5.6 | -5.6 | | 71 | -5.5 | -5.5 | | 119 | -5.2 | -5.9 |
| | 24 | -5.3 | -5.3 | | 72 | -3.7 | -3.5 | | 120 | -7.7 | -6.5 |
| | 25 | -5.3 | -5.5 | | 73 | -5.7 | -4.8 | | 121 | -7.9 | -6.8 |
| | 26 | -4.7 | -6.2 | | 74 | -4.4 | -4.7 | | 122 | -4.2 | -5.1 |
| | 27 | -5.6 | -6.4 | | 75 | -3.3 | -3.0 | | 123 | -4.4 | -5.2 |
| *Millettia griffoniana* | 28 | -7.8 | -8.3 | | 76 | -3.8 | -3.5 | | 124 | -7.9 | -7.4 |
| | 29 | -8.7 | -8.0 | | 77 | -7.1 | -6.5 | | 125 | -7.4 | -6.5 |
| | 30 | -7.8 | -7.6 | | 78 | -5.0 | -4.5 | - | | | |
| | 31 | -7.6 | -7.1 | | 79 | -4.9 | -5.7 | | | | |
| | 32 | -7.5 | -6.8 | | 80 | -4.6 | -4.9 | | | | |
| | 33 | -7.0 | -7.1 | | 81 | -6.9 | -5.5 | | | | |
| | 34 | -7.3 | -7.2 | | 82 | -4.9 | -4.7 | | | | |
| | 35 | -7.4 | -7.3 | | 83 | -5.8 | -6.3 | | | | |
| | 36 | -7.1 | -7.7 | | 84 | -4.6 | -5.4 | | | | |
| | 37 | -7.2 | -8.0 | | 85 | -4.7 | -5.7 | | | | |
| | 38 | -6.9 | -7.2 | | 86 | -5.4 | -5.1 | | | | |
| | 39 | -8.0 | -7.4 | | 87 | -5.2 | -5.7 | | | | |
| | 40 | -7.5 | -8.1 | | 88 | -4.8 | -5.3 | | | | |
| | 41 | -7.2 | -8.0 | | 89 | -7.7 | -7.9 | | | | |
| | 42 | -7.9 | -8.0 | | 90 | -5.4 | -5.8 | | | | |
| | 43 | -7.1 | -6.8 | | 91 | -8.6 | -7.3 | | | | |
| | 44 | -8.2 | -7.5 | | 92 | -6.6 | -6.6 | | | | |
| | 45 | -7.8 | -7.4 | | 93 | -6.9 | -6.5 | | | | |
| | 46 | -6.9 | -6.7 | | 94 | -5.4 | -5.6 | | | | |
| | 47 | -7.1 | -7.2 | | 95 | -4.9 | -4.4 | | | | |
| | 48 | -6.7 | -7.5 | | 96 | -5.3 | -4.7 | | | | |

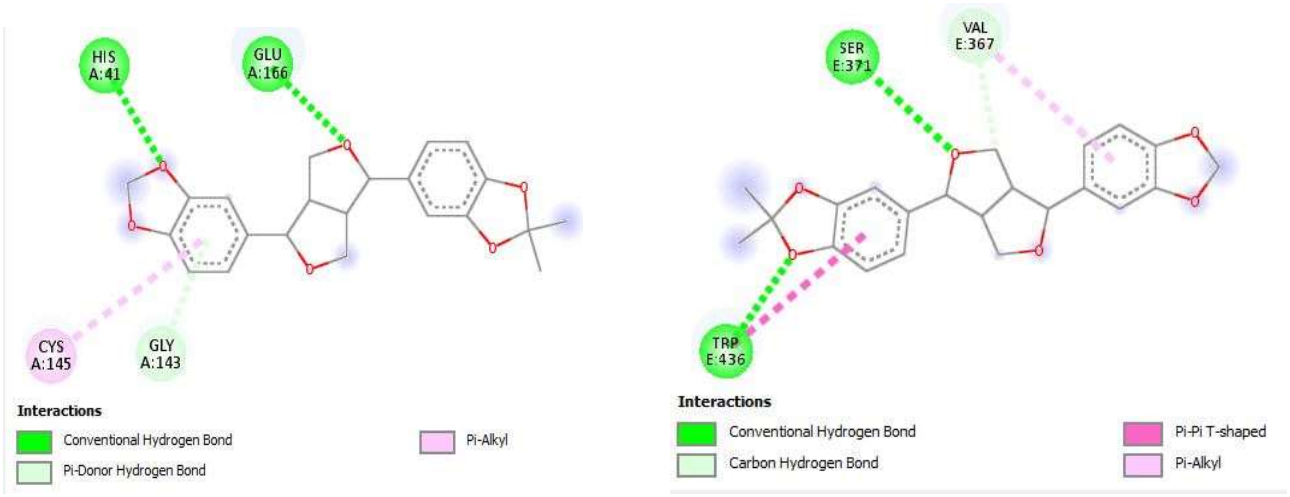


**Fig. 1.** (a) 6lu7-Sesamin interactions. (b) 6m0j-Sesamin interactions.

plants (*M. griffoniana, R. vomitoria, E. globulus,* and *A. montanus*). Then, the evidence database was filtered according to the bioavailability properties of the investigated substances. In this step, drug-like phytochemical profiles were predicted by using the SwissADME online server (http://www.swissadme.ch/index.php ) [43]. In this analysis, the candidates were selected based on the rules of Lipinski, Ghose, Veber, and Egan [52]. Also, other drug-like parameters such as TPSA (Topological Polar Surface Area), number of rotational bonds (nROTB), solubility, and synthetic accessibility (SA) were assessed (Table S2) to evaluate the pharmacodynamics drug profile. Then, we evaluated the pharmacokinetics of phytochemical candidates for bioavailability properties by using the online tool pkCSM [46]. Moreover, the most important pharmacokinetic parameters of the molecules such as absorption, distribution, metabolism, excretion, and toxicity (ADME-Tox) were predicted (Table 2).

**Prediction of molecular drug-like properties.** From Table S2, it can be seen that some phytochemicals belonging to Millettia griffoniana (28, 29, 30, 32, 33, 34, 35, 37, 28, 40, 42, 43, 44, 45, and 48) fulfill all the evaluated bioavailability rules while others (31, 36, 39, 41, and 47) showed numerous violations of Lipinski, Ghose, Veber, and Egan rules.

For the *Rauwolfa vomitoria* phytochemicals (58, 61, 62, and 63), all the evaluated bioavailability conditions are satisfied. However, the phytochemicals (89 and 91) showed some violations of Lipinski's, Ghose's, and Egan's rules, as well as synthetic accessibility difficult (SA > 5).

For *Eucalyptus globulus* phytochemicals, compound 99 fulfilled all evaluated bioavailability parameters whereas others (100, 102, and 105) violate Lipinski, Ghose, Veber. and Egan rules as well as TPSA, SA, and molecular weight (MW).

For phytochemicals from *Acanthus montanus*, all molecules presented multiple violations in bioavailability parameters recommended for molecular structures proposed as drugs.

**Prediction of absorption and distribution properties.** The absorption of a drug determines its local or systemic action. As shown in Table 2, all phytochemicals that fulfill all the evaluated bioavailability rules have an intestinal absorption percentage greater than 92% (92.592 to 99.109%). These lead compounds can cross the membrane of the digestive tract very easily, which involves passive transport because it is non-saturable. Generally, the skin is considered as a protective barrier that acts as a highly impermeable human body region. Nevertheless, in recent times, it is recognized as a specialized organ that aids in the delivery of a wide range of drug molecules into the skin and across the skin into the systemic circulation [51]. According to the skin permeability values obtained (-3.025 to -2.607), these phytochemicals are good candidates for intradermal drug delivery or transdermal drug delivery, since the more negative the $\log K_p$, the less skin permeability of the molecule. As the absorption rate of phytochemical molecules

**Table 2.** Analysis of ADME-Tox Properties (The Phytochemicals Marked in **Bold** have Excellent Pharmacokinetic Properties)

| | Property | | | ADME-Tox report | | | | | | | | | | |
|---|---|---|---|---|---|---|---|---|---|---|---|---|---|---|
| | | | | 32 | **33** | **34** | **35** | 41 | 42 | **43** | **44** | **58** | 62 | 63 | **99** |
| **Absorption** | Human intestinal absorption (% absorbed) | | | 96.06 | 97.029 | 98.894 | 99.82 | 97.651 | 99.091 | 97.441 | 99.109 | 95.623 | 92.592 | 93.699 | 96.275 |
| | Skin permeability ($logk_p$) | | | -2.632 | -2.695 | -2.679 | -2.722 | -2.607 | -2.637 | -2.657 | -2.695 | -2.822 | -2.906 | -3.025 | -2.759 |
| **Distribution** | human VDss ($log\ l\ kg^{-1}$) | | | -0.213 | -0.133 | -0.195 | -0.258 | 0.271 | 0.018 | 0.191 | 0.276 | 1.43 | 1.138 | 1.387 | -0.059 |
| | Human fraction unbound (Fu) | | | 0.186 | 0.218 | 0.211 | 0.167 | 0.197 | 0.231 | 0.196 | 0.199 | 0.23 | 0.292 | 0.232 | 0.044 |
| | BBB permeability (logBB) | | | -0.714 | -0.727 | -0.955 | -0.941 | 0.268 | 0.011 | 0.179 | -0.019 | 0.273 | 0.206 | 0.398 | -0.173 |
| | CNS permeability (logPS) | | | -2.235 | -2.314 | -3.007 | -3.136 | -1.668 | -2.182 | -1.81 | -1.889 | -1.399 | -1.899 | -1.761 | -2.7 |
| **Metabolism** | Cytochrome P450 (CYP450) | Substrate | 2D6 | No | No | No | No | No | No | No | No | Yes | No | No | No |
| | | | 3A4 | Yes | Yes | Yes | Yes | Yes | Yes | Yes | Yes | Yes | Yes | Yes | Yes |
| | | Inhibitor | 1A2 | Yes | Yes | Yes | Yes | Yes | Yes | Yes | Yes | Yes | No | No | Yes |
| | | | 2C19 | Yes | Yes | Yes | Yes | Yes | Yes | Yes | Yes | No | No | No | Yes |
| | | | 2C9 | Yes | Yes | Yes | Yes | Yes | Yes | Yes | Yes | No | No | No | Yes |
| | | | 2D6 | No | No | No | No | No | No | No | No | Yes | No | No | Yes |
| | | | 3A4 | No | Yes | No | Yes | Yes | No | Yes | Yes | No | No | Yes | Yes |
| **Excretion** | Total clearance ($ml\ min^{-1}\ kg^{-1}$) | | | 0.536 | 0.136 | 0.671 | 0.301 | -0.027 | 0.593 | 0.417 | -0.008 | 1.098 | 0.904 | 1.001 | 0.084 |
| **Toxicity** | AMES toxicity | | | Yes | No | No | No | Yes | Yes | No | No | No | No | No | No |
| | Oral rat acute toxicity $LD_{50}$ ($mol\ kg^{-1}$) | | | 2.585 | 2.657 | 2.626 | 2.741 | 2.556 | 2.605 | 2.668 | 3.041 | 2.697 | 2.897 | 2.893 | 2.966 |
| | Oral rat chronic toxicity LOAEL ($log\ mg\ kg^{-1}\_bw/day$) | | | 1.059 | 1.181 | 0.742 | 1.007 | 1.689 | 1.266 | 1.659 | 0.973 | 2.489 | 0.233 | -0.183 | 1.538 |
| | Hepatotoxicity | | | No | No | No | No | Yes | No | No | No | No | Yes | Yes | No |

VDss: Volume of Distribution by the Steady-State method, BBB: Blood-Brain Barrier, CNS: Central Nervous System.

refers to the high absorption through the human intestine (AHI > 90%) as well as the ability of these molecules to permeate the skin (logkp > -2.5) [50], this means that the pharmacokinetics of the phytochemicals examined towards the bloodstream will be excellent and suitable for oral or surface drug use [52].

As the extent of compound distribution and the dose of compounds in the body necessarily affect the compound concentration in plasma and its activity, the distribution properties of our phytochemicals have been predicted. A volume of distribution greater than 1 l $kg^{-1}$ body weight indicates storage or high binding capacity in a body compartment. Except for compounds 58, 62, and 63, all tested phytochemicals had volumes of distribution less than 1 l $kg^{-1}$. In terms of distribution index, the VDss values (logVDss < -0.15) of the phytochemicals (32, 33, 34, and 35) indicate that these molecules were distributed in the plasma. In contrast, the overall higher VDss values for the remaining molecules indicate that they would be distributed in the tissues.

Predicting the fraction unbound in plasma provides a good understanding of the pharmacokinetic properties of a drug to assist candidate selection in the early stages of drug discovery. The unbound fractions of the compounds 33, 34, 43, 58, 62, and 63 were greater than 1/5 (Table 2), yet we know that only this fraction can interact with pharmacological target proteins such as receptors, channels, and enzymes and is able to diffuse between plasma and tissues. Through the fraction of binding molecule-drug-protein parameter at the plasma site, we notice that fraction unbound (FU) values of the examined phytochemicals were less than 0.5. This means that the efficiency of the phytochemicals to cross cell membranes and diffuse will be appropriate [53].

Limited Blood-Brain Barrier (BBB) and Central Nervous System (CNS) permeability protect these organs from exposure to molecules that are toxic to them. All the logPS and the log BB of the phytochemicals 32, 33, 34, 35, 45, and 93 were < 0, showing that only small amounts of these molecules will reach these organic compartments, and we know that a low BBB permeability indicates slow transport into the brain and slow removal from the brain for a compound that has a relatively high brain penetration. The blood-brain barrier (BBB) crossing index indicates that most of the molecules have a value of BBB (logBB < 0.3), with the exception of 63 (logBB = 0.398). This means that the ability of the proposed drug phytochemicals to cross the blood-brain barrier is low, so the use of these molecules as drugs cannot lead to the occurrence of brain-related side effects. Also, the negative logPS values indicate a low ability of the examined molecules to penetrate the central nervous system. Therefore, it is expected that side effects resulting from central nervous system penetration would not occur.

**Prediction of metabolism properties.** CYP450 interacts with several molecules which activate or inhibit enzymatic complex. In adult humans, the three main families of cytochromes involved in the metabolism of many drugs are CYP 1, 2, and 3 and seventy percent of human liver cytochromes are made up of the following seven isoenzymes: CYP 1A2, 2A6, 2B6, 2C, 2D6, 2E1, and 3A [54]. We evaluated cytochrome P450 (CYP) interactions with the investigated candidate drug molecules towards the five cytochromes 1A2, 2C9, 2C19, 2D6, and 3A4 enzymes in drug metabolism in the body [55,56]. The structural diversity of these drug candidates would justify their selectivity of action with the different enzymes of CYP450. In fact, it appears from Table 2 that only 58 can be metabolized by CYP2D6 while all compounds can be oxidized by CYP3A4. Moreover, except 58, 62, and 63, all the phytochemicals inhibit CYP1A2, CYP2C9, and CYP2C19. In the presence of an enzyme inhibitor, drugs metabolized by the inhibited enzyme system have a reduced metabolism, and their plasma elimination half-life increases. The isoform 3A4 is primarily responsible for drug metabolism in the human body. The more the drug acts as a substrate and inhibitor of this enzyme, the safer and less risky the drug will be metabolized [57]. Despite the fact that all the examined molecules act as substrates of the 3A4 enzyme and as inhibitors of the majority of the other cytochrome enzymes, the structure of these molecules is very adapted to the metabolism process in the human body.

**Prediction of excretion properties.** Clearance describes the volume of plasma from which drug would be totally removed per unit time, and the lower the value of the total clearance (log ml $min^{-1}$ $kg^{-1}$), the greater the stability of the drug in the body [50,58]. When a drug has been administered, after its pharmacological effect, it must be eliminated and knowledge of the clearance of each potential drug

is a key step in its development. The total clearance (log ml $min^{-1}$ $kg^{-1}$) of 42 and 45 were < 0, showing that the half-life of these two phytochemicals is greater than the others. Nevertheless, it has been seen that each compound could be metabolized by at least one isoform of CYP450, which would increase its solubility as well as its excretion. The total clearance of most assayed compounds showed their ability to be easily eliminated from the body, thus preventing the organism from the undesirable effects linked to drug accumulation.

## Toxicity Pattern Analysis of Top Drug Candidates

Based on the ADME properties of the investigated phytochemicals, it appears that these molecules have very favorable ADME properties for medicinal use. However, the knowledge of the toxicological profile of these phytochemicals is of great importance, especially for the liver and undesired lethal doses. Therefore, we added another evaluation that included the toxicity of these molecules in terms of AMES test, Acute Oral Rat Toxicity ($LD_{50}$), Chronic Rat Oral Toxicity (LOAEL), and Hepatotoxicity (Table 2). Since the higher the $LD_{50}$, the lower the acute toxicity, we can say that these potential drugs would not be responsible for acute poisoning given their high $LD_{50}$ (2.556 to 3.041 mol $kg^{-1}$). Concerning the lowest observed adverse effect level (LOAEL), it is defined as the lowest dose where the effects observed in the treated group imply an adverse effect on the subject. We can understand by this definition that the higher it is, the less the compound will cause chronic intoxication. Thus, compounds with low LOAEL (34, 62, and 63) are more susceptible to chronic intoxication. For such compounds, micromolar or nanomolar doses are recommended to achieve therapeutic efficacy and suitability. The AMES test and hepatotoxicity evaluations indicated that the structures of phytochemicals 32, 42, 43, 62, and 63 may be responsible for hepatotoxicity or other forms of unpleasant side effects. Thus, we exclude these molecules from the list of candidates for suitable drug application.

## Osiris Calculations/Toxicity Risks

Based on Osiris predictions, we exclude the phytochemicals that pose the greatest risk of toxicity, while keeping the safest (not toxic) phytochemicals. To further support the screening of candidate phytochemicals for medicinal use against SARS-CoV-2, we predict the toxicity risks of these candidate phytochemicals. To do this, we filtered the selected drug-like molecules for Osiris computations [59,60]. During this prediction procedure, potential toxicity risks were evaluated to be mutagenic, tumorigenic, irritant, and reproductive (Table 3).

In Table 3, phytochemicals 28, 29, 30, 37, 38, 40, and 48 from *Millettia griffoniana* present toxicity risks that can produce carcinogenic side effects, irritations, and reproduction problems. Also, the phytochemical 61 from *Rauwolfa vomitoria* can produce irritant side effects while the phytochemicals 32, 33, 34, 35, 42, 43, 44, 45, 58, 62, 63, and 93 did not show any potential toxicity risks. Therefore, we can adopt this phytochemical as the best drug candidate against SARS-CoV-2 infection.

Phytochemicals not fulfilling the evaluated parameters were excluded based on drug-like bioavailability parameter predictions. However, we select phytochemicals that met all the bioavailability conditions suitable for oral drug use. Pharmacokinetics and bioavailability of phytopharmaceuticals predictions for each molecule proved that the phytochemicals 32, 33, 34, 35, 42, 43, 44, 45, 58, 62, 63, and 93 derived from the plants, *Millettia griffoniaana, Rauwolfa vomitoria,* and *Eucalyptus globulus*, are suitable for safe drug use.

## Molecular Dynamics Results

**Analysis of RMSD and RMSF.** Primarily, the stability of the investigated systems (6lu7 alone and its complex with sesamin) was studied by analyzing the variation of their RMSD values over the simulation period. The RMSD plots corresponding to 6lu7 alone and 6lu7-sesamin complex are shown in Fig. 2a. According to the obtained results, the RMSD of the 6lu7-sesamin complex fluctuated till reaching to a steady state after 50 ns, while the RMSD trajectory corresponding to 6lu7 alone was relatively stable since the beginning of the simulation. Overall, the RMSD graph indicates that the ligand (sesamin) disturbed the protein conformation at the beginning of the simulation, but after a few nanoseconds, it turned out that it stabilized at the active site of the target protein. Besides, the RMSF values corresponding to Cα atoms of the target protein in un-complexed and complexed forms were calculated to gain insight into the fluctuation degree of the protein residues

**Table 3.** Osiris Predictions of Phytochemical Toxicity Risks

| Phytochemicals class | Com. | Toxicity risks | | | |
|---|---|---|---|---|---|
| | | MUT | TUMO | IRRI | REP |
| Millettia griffoniana | **28** | | | | |
| | **29** | | | | |
| | **30** | | | | |
| | 32 | | | | |
| | 33 | | | | |
| | 34 | | | | |
| | 35 | | | | |
| | **37** | | | | |
| | **38** | | | | |
| | **40** | | | | |
| | 42 | | | | |
| | 43 | | | | |
| | 44 | | | | |
| | 45 | | | | |
| | **48** | | | | |
| Rauwolfa vomitoria | 58 | | | | |
| | **61** | | | | |
| | 62 | | | | |
| | 63 | | | | |
| **Eucalyptus globulus** | 93 | | | | |

Phytochemicals in **bold** show potential toxicity risks

MUT: *mutagenic*; TUM: *tumorigenic*; IRRIT: *irritant*; RE: *reproductive* effective

: Not toxic : Toxic : Slightly toxic

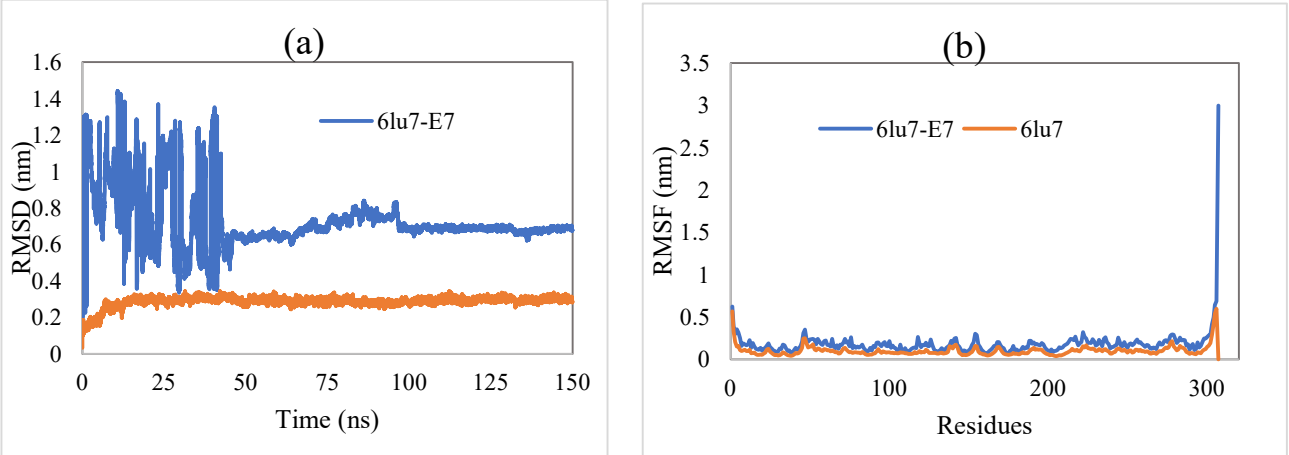


**Fig. 2.** (a) Root mean square deviation (RMSD) of the backbone of 6lu7 and 6lu7-sesamin (6lu7-E7) complex as a function of time. (b) Root mean square fluctuation (RMSF) of Cα atoms of 6lu7 in the absence and presence of sesamin (E7).

(Fig. 2b). From Fig. 2b, we note that the RMSF value of most of the amino acids of 6lu7 was found to be lower than 0.2 nm, signifying the great stability of the studied systems. The average values of RMSF corresponding to 6lu7 and its complex were found to be 0.100 and 0.184 nm, respectively. Furthermore, the RMSF plots corresponding to the 6lu7 un-complexed and complexed adopt similar profiles, indicating that sesamin did not influence the flexibility of the protein residues [61].

**Assessment of Rg and SASA.** The radius of gyration ($R_g$) defined as the mass-weighted RMS distance of a collection of atoms from their common center of mass, is another parameter used to study the stability of proteins in an aqueous medium [62,63]. Figure 3a shows the $R_g$ plots corresponding to the 6lu7 and 6lu7- sesamin complex. The average $R_g$ of the 6lu7 and 6lu7-sesamin complex was found to be 2.223 and 2.239 nm, respectively. In addition, $R_g$ of 6lu7-sesamin variates until reaching a steady state after 50 ns, showing the stability of the investigated complex in the aqueous environment. Overall, the trajectory of $R_g$ exhibited by 6lu7-sesamin indicates that 6lu7 was in an expanded form and transitioned to a stable and more compact form due to its interactions with sesamin. Besides, the change in the protein surface area was also described by studying the Solvent accessible surface area (SASA). Figure 3b illustrates the SASA plots corresponding to 6lu7 and its complex. The average SASA of 6lu7 and 6lu7-sesamin was found to be 148.774 and 151.358 $nm^2$, respectively. These values indicate that there are negligible changes in the surface area of 6lu7 induced by its interactions with sesamin. In addition, we note that the SASA of 6lu7-sesamin exhibited some initial variations until reaching a stable state after 50 ns, confirming the stability of the studied systems. Furthermore, the high values of solvent-accessible surface area exhibited by 6lu7 complexed with sesamin, before reaching the steady state, confirm that 6lu7 was at the expanded form and then it transitioned to compact form due to its interactions with sesamin, as described by $R_g$ trajectory.

**Analysis of hydrogen bonds.** The number of hydrogen bonds implicated between the sesamin and 6lu7 was also analyzed during the simulation time (Fig. 3). From Fig. 4, we note that sesamin was able to form hydrogen bonds with the 6lu7 only after almost 45 ns, which explains the stability of the studied complex after some initial variations as expressed by the investigated parameters (RMSD, $R_g$, and SASA). Therefore, the involvement of hydrogen bonds is a critical

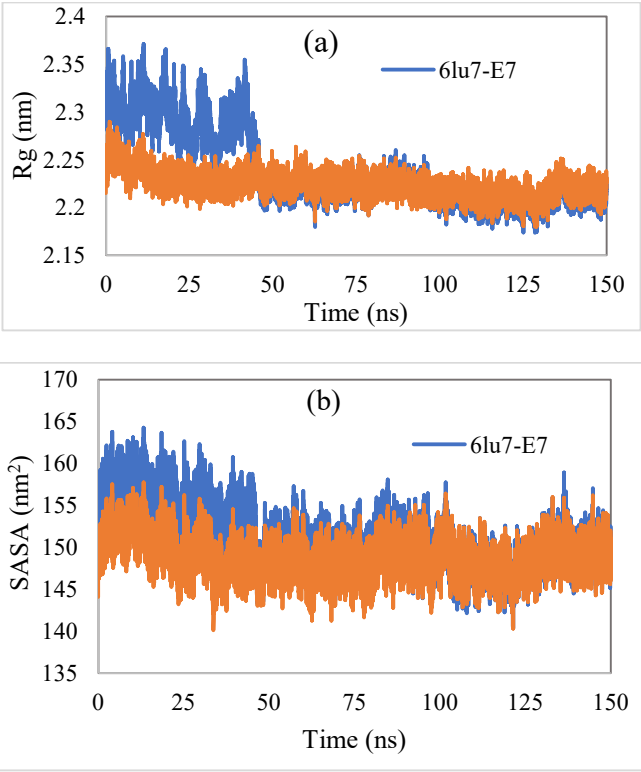


**Fig. 3.** (a) Radius of gyration (Rg) of 6lu7 and 6lu7-sesamin (6lu7-E7) complex as a function of time. (b) Solvent accessible surface area (SASA) of 6lu7 and 6lu7-sesamin (6lu7-E7) complex.

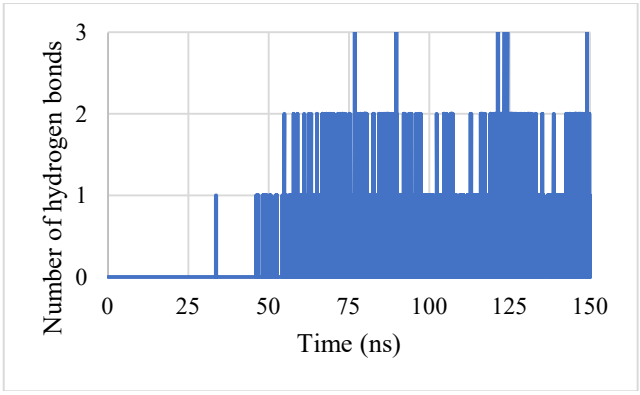


**Fig. 4.** The number of hydrogens formed by sesamin with 6lu7 as a function of time.

factor for the stability of the 6lu7-sesamin complex. Indeed, the ability of several poses of sesamin to implicate hydrogen bonds with 6lu7 lead to a stable complex.

## CONCLUSIONS

The results of the drug-like evaluation indicate that the phytochemicals belonging to *Acanthus montanus* investigated in this study are inappropriate candidates for drugs. All pharmacokinetics, bioavailability, and toxicity predictions for each phytochemical demonstrated that the phytochemicals maximaisoflavone G, 7-hydroxy-6-methoxy-3',4'-methylenedioxyisoflavone, maximaisoflavone G acetate, 7-acetoxy-6-methoxy-3',4'-methylenedioxy-isoflavone, calapogonium isoflavone, 7-2'-dimethoxy-4',5'-methylenedioxy isoflavone, jamaicin, durmillone, normacusine B, geissoschizine, tetrahydroalstonine, and sesamin are suitable for safe drug use. Thus, these phytochemicals can be used to design new drugs against SARS-CoV-2 $M^{pro}$ and spike proteins.

## REFERENCES


[1] Huang, C.; Wang, Y.; Li, X.; Ren, L.; Zhao, J.; Hu, Y.; Zhang, L.; Fan, G.; Xu, J.; Gu, X., Clinical Features of Patients Infected with 2019 Novel Coronavirus in Wuhan. *China*. *The Lancet.* **2020**, *395*, 497-506, DOI: 10.1016/S0140-6736(20)30183-5.

[2] *WHO Coronavirus (COVID-19) Dashboard*. https://covid19.who.int (accessed 2022-06-26).

[3] Mortola, E.; Roy, P., Efficient Assembly and Release of SARS Coronavirus-like Particles by a Heterologous Expression System. *FEBS Lett.* **2004**, *576*, 174-178, DOI: 10.1016/j.febslet.2004.09.009.

[4] Wang, C.; Zheng, X.; Gai, W.; Zhao, Y.; Wang, H.; Wang, H.; Feng, N.; Chi, H.; Qiu, B.; Li, N., MERS-CoV Virus-like Particles Produced in Insect Cells Induce Specific Humoural and Cellular Imminity in Rhesus Macaques. *Oncotarget.* **2017**, *8*, 12686, DOI: 10.18632/oncotarget.8475.

[5] De, P.; Roy, K., Computational Modeling of ACE2-Mediated Cell Entry Inhibitors for the Development of Drugs Against Coronaviruses. *Methods Pharmacol. Toxicol.* **2021**, 495-539, DOI: 10.1007/7653_2020_49.

[6] Siu, Y. L.; Teoh, K. T.; Lo, J.; Chan, C. M.; Kien, F.; Escriou, N.; Tsao, S. W.; Nicholls, J. M.; Altmeyer, R.; Peiris, J. S. M., The M, E, and N Structural Proteins of the Severe Acute Respiratory Syndrome Coronavirus Are Required for Efficient Assembly, Trafficking, and Release of Virus-like Particles. *J. Virol.* **2008**, *82*, 11318-11330, DOI: 10.1128/JVI.01052-08.

[7] Song, H. C.; Seo, M. -Y.; Stadler, K.; Yoo, B. J.; Choo, Q. -L.; Coates, S. R.; Uematsu, Y.; Harada, T.; Greer, C. E.; Polo, J. M., Synthesis and Characterization of a Native, Oligomeric Form of Recombinant Severe Acute Respiratory Syndrome Coronavirus Spike Glycoprotein. *J. Virol.* **2004**, *78*, 10328-10335, DOI: 10.1128/JVI.78.19.10328-10335.2004.

[8] Kirchdoerfer, R. N.; Cottrell, C. A.; Wang, N.; Pallesen, J.; Yassine, H. M.; Turner, H. L.; Corbett, K. S.; Graham, B. S.; McLellan, J. S.; Ward, A. B., Pre-Fusion Structure of a Human Coronavirus Spike Protein. *Nature.* **2016**, *531*, 118-121, DOI: 10.1038/nature17200.

[9] Neuman, B. W.; Kiss, G.; Kunding, A. H.; Bhella, D.; Baksh, M. F.; Connelly, S.; Droese, B.; Klaus, J. P.; Makino, S.; Sawicki, S. G., A Structural Analysis of M Protein in Coronavirus Assembly and Morphology. *J. Struct. Biol.* **2011**, *174*, 11-22, DOI: 10.1016/j.jsb.2010.11.021.

[10] Masters, P. S., The Molecular Biology of Coronaviruses. *Adv. Virus Res.* **2006**, *66*, 193-292, DOI: 0.1016/S0065-3527(06)66005-3.

[11] Fehr, A. R.; Perlman, S., Coronaviruses: An Overview of Their Replication and Pathogenesis. *Coronaviruses* **2015**, *1282*, 1-23, DOI: 10.1007/978-1-4939-2438-7_1.

[12] Opstelten, D. J.; Raamsman, M. J.; Wolfs, K.; Horzinek, M. C.; Rottier, P. J., Envelope Glycoprotein Interactions in Coronavirus Assembly. *J. Cell Biol.* **1995**, *131*, 339-349, DOI: 10.1083/jcb.131.2.339.

[13] Fouedjou, R. T.; Chtita, S.; Bakhouch, M.; Belaidi, S.; Ouassaf, M.; Djoumbissie, L. A.; Tapondjou, L. A.; Abul Qais, F., Cameroonian Medicinal Plants as Potential Candidates of SARS-CoV-2 Inhibitors. *J. Biomol. Struct. Dyn.* **2021**, 1-15, DOI: 10.1080/07391102.2021.1914170.

[14] Craik, D. J.; Fairlie, D. P.; Liras, S.; Price, D., The Future of Peptide-Based Drugs. *Chem. Biol. Drug Des.*

**2013**, *81*, 136-147, DOI: 10.1111/cbdd.12055.

[15] Niemirski, R.; Zych, M., Fly Pollination of Dichogamous Angelica Sylvestris (Apiaceae): How (Functionally) Specialized Can a (Morphologically) Generalized Plant Be? *Plant Syst. Evol.* **2011**, *294*, 147-158, DOI: 10.1007/s00606-011-0454-y.

[16] Speizer, F. E.; Colditz, G. A.; Hunter, D. J.; Rosner, B.; Hennekens, C., Prospective Study of Smoking, Antioxidant Intake, and Lung Cancer in Middle-Aged Women (USA). *Cancer Causes Control.* **1999**, *10*, 475-482, DOI: 10.1023/A:1008931526525.

[17] Hosseinzadeh, H.; Nassiri-Asl, M., Avicenna's (Ibn Sina) the Canon of Medicine and Saffron (Crocus Sativus): A Review. *Phytother. Res.* **2013**, *27*, 475-483, DOI: 10.1002/ptr.4784.

[18] Thomford, N. E.; Dzobo, K.; Chopera, D.; Wonkam, A.; Skelton, M.; Blackhurst, D.; Chirikure, S.; Dandara, C., Pharmacogenomics Implications of Using Herbal Medicinal Plants on African Populations in Health Transition. *Pharmaceuticals*. **2015**, *8*, 637-663, DOI: 10.3390/ph8030637.

[19] Ena, R.; Rath, D.; Rout, S. S.; Kar, D. M., A Review on Genus Millettia: Traditional Uses, Phytochemicals and Pharmacological Activities. *Saudi Pharm. J*. **2020**, *28*, 1686-1703, DOI: 10.1016/j.jsps.2020.10.015.

[20] Titanji, V. P.; Zofou, D.; Ngemenya, M. N., The Antimalarial Potential of Medicinal Plants Used for the Treatment of Malaria in Cameroonian Folk Medicine. *Afr. J. Tradit. Complement. Altern. Med.* **2008**, *5*, 302, PMCID: PMC2816552.

[21] Adegoke, G. O.; Skura, B. J., Nutritional Profile and Antimicrobial Spectrum of the SpiceAframomum Danielli K. Schum. *Plant Foods Hum. Nutr.* **1994**, *45*, 175-182, DOI: 10.1007/BF01088475.

[22] Adegoke, G. O.; Iwahashi, H.; Komatsu, Y.; Obuchi, K.; Iwahashi, Y., Inhibition of Food Spoilage Yeasts and Aflatoxigenic Moulds by Monoterpenes of the Spice Aframomum Danielli. *Flavour Fragr. J.* **2000**, *15*, 147-150, DOI: 10.1002/1099-1026(200005/06)15:3<147::AID-FFJ883>3.0.CO;2-0.

[23] Adegoke, G.; Gbadamosi, R.; Evwoerhurhoma, F.; Uzo-peters, P.; Falade, K.; Itiola, O.; Moody, O.; Skura, B., Protection of Maize (Zea Mays) and Soybeans (Glycine Max) Using Aframomum Danielli. *Eur. Food Res. Technol.* **2002**, *214*, 408-411, DOI: 10.1007/s00217-001-0476-8.

[24] Pavela, R.; Maggi, F.; Mbuntcha, H.; Woguem, V.; Fogang, H. P. D.; Womeni, H. M.; Tapondjou, L. A.; Barboni, L.; Nicoletti, M.; Canale, A., Traditional Herbal Remedies and Dietary Spices from Cameroon as Novel Sources of Larvicides against Filariasis Mosquitoes? *Parasitol. Res.* **2016**, *115*, 4617-4626, DOI: 10.1007/s00436-016-5254-4.

[25] Adegoke, G. O.; Gopala Krishna, A. G., Extraction and Identification of Antioxidants from the Spice Aframomum Danielli. *J. Am. Oil Chem. Soc.* **1998**, *75*, 1047-1052, DOI: 10.1007/s11746-998-0285-3.

[26] Akpanabiatu, M. I., Effects of the Biochemical Interactions of Vitamins A and E on the Toxicity of Root Bark Extract of Rauwolfia Vomitoria (Apocynaceae) in Wistar Albino Rats. *PhD Univ. Calabar Calabar Niger.* **2006**.

[27] Yaniv, Z.; Bachrach, U., Handbook of Medicinal Plants. *CRC Pres.* **2005**, 522p.

[28] Amole, O. O.; Yemitan, O. K.; Oshikoya, K. A., Anticonvulsant Activity of Rauvolfia Vomitoria (Afzel). *Afr. J. Pharm. Pharmacol.* **2009**, *3*, 319-322, DOI: 10.5897/AJPP.9000044.

[29] Bisong, S. A.; Brown, R.; Osim, E. E., Comparative Effects of Rauwolfia Vomitoria and Chlorpromazine on Locomotor Behaviour and Anxiety in Mice. *J. Ethnopharmacol.* **2010**, *132*, 334-339, DOI: 10.1016/j.jep.2010.08.045.

[30] Bisong, S.; Brown, R.; Osim, E., Comparative Effects of Rauwolfia Vomitoria and Chlorpromazine on Social Behaviour and Pain. *North Am. J. Med. Sci.* **2011**, *3*, 48-54, DOI: 10.4297/najms.2011.348.

[31] Boulekbache-Makhlouf, L.; Meudec, E.; Chibane, M.; Mazauric, J.-P.; Slimani, S.; Henry, M.; Cheynier, V.; Madani, K., Analysis by High-Performance Liquid Chromatography Diode Array Detection Mass Spectrometry of Phenolic Compounds in Fruit of Eucalyptus Globulus Cultivated in Algeria. *J. Agric. Food Chem.* **2010**, *58*, 12615-12624, DOI: 10.1021/jf1029509.

[32] Boulekbache-Makhlouf, L.; Slimani, S.; Madani, K., Total Phenolic Content, Antioxidant and Antibacterial Activities of Fruits of Eucalyptus Globulus Cultivated

in Algeria. *Ind. Crops Prod.* **2013**, *41*, 85-89, DOI: 10.1016/j.indcrop.2012.04.019.

[33] Chinnarasu, C.; Montes, A.; Fernandez-Ponce, M. T.; Casas, L.; Mantell, C.; Pereyra, C.; de la Ossa, E. M.; Pattabhi, S., Natural Antioxidant Fine Particles Recovery from Eucalyptus Globulus Leaves Using Supercritical Carbon Dioxide Assisted Processes. *J. Supercrit. Fluids* **2015**, *101*, 161-169, DOI: 10.1016/j.supflu.2015.03.013.

[34] Harkat-Madouri, L.; Asma, B.; Madani, K.; Bey-Ould Si Said, Z.; Rigou, P.; Grenier, D.; Allalou, H.; Remini, H.; Adjaoud, A.; Boulekbache-Makhlouf, L., Chemical Composition, Antibacterial and Antioxidant Activities of Essential Oil of Eucalyptus Globulus from Algeria. *Ind. Crops Prod.* **2015**, *78*, 148-153, DOI: 10.1016/j.indcrop.2015.10.015.

[35] Jagtap, U. B.; Bapat, V. A., Artocarpus: A Review of Its Traditional Uses, Phytochemistry and Pharmacology. *J. Ethnopharmacol.* **2010**, *129*, 142-166, DOI: 10.1016/j.jep.2010.03.031.

[36] Noumi, E.; Fozi, F. L., Ethnomedical Botany of Epilepsy Treatment in Fongo-Tongo Village, Western Province, Cameroon. *Pharm. Biol.* **2003**, *41*, 330-339, DOI: 10.1076/phbi.41.5.330.15944.

[37] Jin, Z.; Du, X.; Xu, Y.; Deng, Y.; Liu, M.; Zhao, Y.; Zhang, B.; Li, X.; Zhang, L.; Peng, C.; Duan, Y.; Yu, J.; Wang, L.; Yang, K.; Liu, F.; Jiang, R.; Yang, X.; You, T.; Liu, X.; Yang, X.; Bai, F.; Liu, H.; Liu, X.; Guddat, L. W.; Xu, W.; Xiao, G.; Qin, C.; Shi, Z.; Jiang, H.; Rao, Z.; Yang, H., Structure of Mpro from SARS-CoV-2 and Discovery of Its Inhibitors. *Nature.* **2020**, *582*, 289-293, DOI: 10.1038/s41586-020-2223-y.

[38] Chtita, S.; Belhassan, A.; Aouidate, A.; Belaidi, S.; Bouachrine, M.; Lakhlifi, T., Discovery of Potent SARS-CoV-2 Inhibitors from Approved Antiviral Drugs via Docking and Virtual Screening. *Comb. Chem. High Throughput Screen.* **2021**, *24*, 441-454, DOI: 10.2174/1386207323999200730205447.

[39] Dakam, W.; Nguemfo, E. L.; Fannang, S. V.; Azombo, E. L. A.; Ndomou, M., Safety Assessment of Glyphaea Brevis Spreng. (Tiliaceae): Acute and Subacute Toxicity of the Leaf Aqueous Extract in Mice and Wistar Rats. *J. Drug Deliv. Ther.* **2022**, *12*, 77-85, DOI: 10.22270/jddt.v12i2-S.5269.

[40] Milani, M.; Donalisio, M.; Bonotto, R. M.; Schneider, E.; Arduino, I.; Boni, F.; Lembo, D.; Marcello, A.; Mastrangelo, E., Combined in Silico and in Vitro Approaches Identified the Antipsychotic Drug Lurasidone and the Antiviral Drug Elbasvir as SARS-CoV2 and HCoV-OC43 Inhibitors. *Antiviral Res.* **2021**, *189*, 105055, DOI: 10.1016/j.antiviral.2021.105055.

[41] Saqrane, S.; El Mhammedi, M. A.; Lahrich, S.; Laghrib, F.; El Bouabi, Y.; Farahi, A.; Bakasse, M., Recent Knowledge in Favor of Remdesivir (GS-5734) as a Therapeutic Option for the COVID-19 Infections. *J. Infect. Public Health.* **2021**, *14,* 655-660, DOI: 10.1016/j.jiph.2021.02.006.

[42] Morris, G. M.; Huey, R.; Lindstrom, W.; Sanner, M. F.; Belew, R. K.; Goodsell, D. S.; Olson, A. J., AutoDock4 and AutoDockTools4: Automated Docking with Selective Receptor Flexibility. *J. Comput. Chem.* **2009**, *30*, 2785-2791, DOI: 10.1002/jcc.21256.

[43] Daina, A.; Michielin, O.; Zoete, V., SwissADME: A Free Web Tool to Evaluate Pharmacokinetics, Drug-Likeness and Medicinal Chemistry Friendliness of Small Molecules. *Sci. Rep.* **2017**, *7*, 42717, DOI: 10.1038/srep42717.

[44] Kar, B.; Dehury, B.; Singh, M. K.; Pati, S.; Bhattacharya, D., Identification of Phytocompounds as Newer Antiviral Drugs against COVID-19 through Molecular Docking and Simulation Based Study. *J. Mol. Graph. Model.* **2022**, *114*, 108192, DOI: 10.1016/j.jmgm.2022.108192.

[45] Al-Shuhaib, M. B. S.; Hashim, H. O.; Al-Shuhaib, J. M., Epicatechin Is a Promising Novel Inhibitor of SARS-CoV-2 Entry by Disrupting Interactions between Angiotensin-Converting Enzyme Type 2 and the Viral Receptor Binding Domain: A Computational/Simulation Study. *Comput. Biol. Med.* **2022**, *141*, 105155, DOI: 10.1016/j.compbiomed.2021.105155.

[46] Pires, D. E. V.; Blundell, T. L.; Ascher, D. B., PkCSM: Predicting Small-Molecule Pharmacokinetic and Toxicity Properties Using Graph-Based Signatures. *J. Med. Chem.* **2015**, *58*, 4066-4072, DOI: 10.1021/acs.jmedchem.5b00104.

[47] Parhi, R.; Mandru, A., Enhancement of Skin Permeability with Thermal Ablation Techniques:

Concept to Commercial Products. *Drug Deliv. Transl. Res.* **2021**, *11*, 817-841, DOI: 10.1007/s13346-020-00823-3.

[48] Van Der Spoel, D.; Lindahl, E.; Hess, B.; Groenhof, G.; Mark, A. E.; Berendsen, H. J., GROMACS: Fast, Flexible, and Free. *J. Comput. Chem.* **2005**, *26* (16), 1701-1718, DOI: 10.1002/JCC.20291.

[49] Bjelkmar, P.; Larsson, P.; Cuendet, M. A.; Hess, B.; Lindahl, E., Implementation of the CHARMM Force Field in GROMACS: Analysis of Protein Stability Effects from Correction Maps, Virtual Interaction Sites, and Water Models. *J. Chem. Theory Comput.* **2010**, *6* (2), 459-466, DOI: 10.1021/CT900549R.

[50] Zoete, V.; Cuendet, M. A.; Grosdidier, A.; Michielin, O., SwissParam: A Fast Force Field Generation Tool for Small Organic Molecules. *J. Comput. Chem.* **2011**, *32* (11), 2359-2368, DOI: 10.1002/jcc.21816.

[51] Parrinello, M.; Rahman, A., Polymorphic Transitions in Single Crystals: A New Molecular Dynamics Method. *J. Appl. Phys.* **1981**, *52* (12), 7182-7190, DOI: 10.1063/1.328693.

[52] Daoui, O.; Mazoir, N.; Bakhouch, M.; Salah, M.; Benharref, A.; Gonzalez-Coloma, A.; Elkhattabi, S.; Yazidi, M. E.; Chtita, S., 3D-QSAR, ADME-Tox, and Molecular Docking of Semisynthetic Triterpene Derivatives as Antibacterial and Insecticide Agents. *Struct. Chem.* **2022**, 33, 1063–1084, DOI: 10.1007/s11224-022-01912-4.

[53] Watanabe, R.; Esaki, T.; Kawashima, H.; Natsume-Kitatani, Y.; Nagao, C.; Ohashi, R.; Mizuguchi, K., Predicting Fraction Unbound in Human Plasma from Chemical Structure: Improved Accuracy in the Low Value Ranges. *Mol. Pharm.* **2018**, *15*, 5302-5311, DOI: 10.1021/acs.molpharmaceut.8b00785.

[54] Bernhardt, R., Cytochrome P450: Structure, Function, and Generation of Reactive Oxygen Species. In *Reviews of Physiology Biochemistry and Pharmacology.* **1996**, *127*, 137-221, DOI: 10.1007/BFb0048267.

[55] Daoui, O.; Elkhattabi, S.; Chtita, S.; Elkhalabi, R.; Zgou, H.; Benjelloun, A. T., QSAR, Molecular Docking and ADMET Properties in Silico Studies of Novel 4,5, 6,7-Tetrahydrobenzo [D]-Thiazol-2-Yl Derivatives Derived from Dimedone as Potent Anti-Tumor Agents through Inhibition of C-Met Receptor Tyrosine Kinase. *Heliyon.* **2021**, *7*, e07463, DOI: 10.1016/j.heliyon.2021.e07463.

[56] Larik, F. A.; Faisal, M.; Saeed, A.; Channar, P. A.; Korabecny, J.; Jabeen, F.; Mahar, I. A.; Kazi, M. A.; Abbas, Q.; Murtaza, G.; Khan, G. S.; Hassan, M.; Seo, S. -Y., Investigation on the Effect of Alkyl Chain Linked Mono-Thioureas as Jack Bean Urease Inhibitors, SAR, Pharmacokinetics ADMET Parameters and Molecular Docking Studies. *Bioorganic Chem.* **2019**, *86*, 473-481, DOI: 10.1016/j.bioorg.2019.02.011.

[57] Winiwarter, S.; Ahlberg, E.; Watson, E.; Oprisiu, I.; Mogemark, M.; Noeske, T.; Greene, N., In Silico ADME in Drug Design-Enhancing the Impact. *ADMET DMPK.* **2018**, *6*, 15-33, DOI: 10.5599/admet.6.1.470.

[58] Szakács, G.; Váradi, A.; Özvegy-Laczka, C.; Sarkadi, B., The Role of ABC Transporters in Drug Absorption, Distribution, Metabolism, Excretion and Toxicity (ADME-Tox). *Drug Discov. Today.* **2008**, *13*, 379-393, https://doi.org/10.1016/j.drudis.2007.12.010.

[59] Rbaa, M.; Haida, S.; Tuzun, B.; hichar, A.; Hassane, A. E.; Kribii, A.; Lakhrissi, Y.; Hadda, T. B.; Zarrouk, A.; Lakhrissi, B.; Berdimurodov, E., Synthesis, Characterization and Bioactivity of Novel 8-Hydroxyquinoline Derivatives: Experimental, Molecular Docking, DFT and POM Analyses. *J. Mol. Struct.* **2022**, *1258*, 132688, DOI: 10.1016/j.molstruc.2022.132688.

[60] Bououden, W.; Benguerba, Y., Computational Quantum Chemical Study, Drug-Likeness and In Silico Cytotoxicity Evaluation of Some Steroidal Anti-Inflammatory Drugs. *J. Drug Deliv. Ther.* **2020**, *10*, 68-74, DOI: 10.22270/jddt.v10i3-s.4165.

[61] Nour, H.; Abdou, A.; Belaidi, S .; JamalEddine, J.; Elmakssoudi, A.; Dakir, M.; Chtita, S., Discovery of promising cholinesterase inhibitors for Alzheimer's disease treatment through DFT, docking, and molecular dynamics studies of eugenol derivatives. *J. Chinese Chem. Soc.* **2022**, DOI: 10.1002/JCCS.202200195.

[62] Nour, H.; Abchir, O.; Belaidi, S.; Qais, F. A.; Chtita, S.; Belaaouad, S. 2D-QSAR and Molecular Docking Studies of Carbamate Derivatives to Discover Novel Potent Anti-Butyrylcholinesterase Agents for Alzheimer's Disease Treatment. *Bull. Korean Chem.*

*Soc.* **2022**, *43* (2), 277-292, DOI: 10.1002/BKCS.12449.

[63] Daoui, O.; Elkhattabi, S.; Chtita, S., Rational Design of Novel Pyridine-Based Drugs Candidates for Lymphoma Therapy. *J. Mol. Struct.* **2022**, *1270*, 133964, DOI: 10.1016/j.molstruc.2022.133964.